

Pressure dependence of phonons in Rb_4C_{60} studied with Raman spectroscopy

Ch. Bellin and J. C. Chervin

Institut de Minéralogie et Physique de la Matière Condensée, Université Paris VI, UMR CNRS 7590, case 115, 4 pl. Jussieu, 75252 Paris Cedex 05, France

C. Hérold

Laboratoire de Chimie du Solide Minéral, Université Henri Poincaré Nancy I, Boîte Postale 239, 54506 Vandoeuvre lès Nancy Cedex, France

N. Bendiab

Institut de Minéralogie et Physique de la Matière Condensée, Université Paris VI, UMR CNRS 7590, case 115, 4 pl. Jussieu, 75252 Paris Cedex 05, France and Laboratoire de Spectrométrie Physique, Université Joseph Fourier, 140 Avenue de la physique, Boîte Postale 87, 38402 Saint Martin d'Hères Cedex, France

(Received 26 October 2007; revised manuscript received 12 March 2008; published 5 June 2008)

Raman spectra of Rb_4C_{60} have been measured as a function of pressure up to 8 GPa at room temperature. Intramolecular modes exhibit three remarkable changes around 0.6, 1.7, and 4 GPa. An increase in the pressure slopes of various mode frequencies occurs at 0.6 GPa. Then an overall decrease in the pressure slopes occurs around 1.7 GPa. Finally, we observe the new lines appearing around 4 GPa. These effects are discussed in terms of reduction in the symmetry of the C_{60} molecule and electron hopping.

DOI: [10.1103/PhysRevB.77.245409](https://doi.org/10.1103/PhysRevB.77.245409)

PACS number(s): 71.20.Tx, 74.62.Fj, 78.30.-j

I. INTRODUCTION

The alkali doped $A_n\text{C}_{60}$ (A is the alkali) has been a topic of large interest mainly due to the diversity of their structural and electronic properties. The phase $n=3$ is metallic and superconducting with a fcc crystal lattice. The phase $n=6$ is insulating with a bcc lattice. The case of the bct phase $n=4$ puzzles the fullerene community.¹ $A_4\text{C}_{60}$ compounds are nonmagnetic narrow-gap semiconductors at ambient pressure, as evidenced by NMR² and photoemission³ experiments. Sophisticated calculations such as density-functional or tight-binding Hartree-Fock calculations predicted them to be respectively metallic^{4,5} or to be wide-gap insulators⁵ while the experiments indicate them as a narrow-gap semiconductor⁶ so that the Jahn-Teller effect has been consensually invoked.^{5,6}

$A_4\text{C}_{60}$ compounds undergo an insulator to metal transition under pressure around 0.8 GPa, as evidenced by NMR on Rb_4C_{60} (Ref. 7) performed up to 1.2 GPa. Diffraction experiment evidenced an abrupt compressibility jump between 0.5 and 0.8 GPa that was attributed to a structural phase transition preserving the tetragonal symmetry⁸ or leading to an ordered orthorhombic structure.⁹ To go further, the electronic density modification under pressure has been studied by inelastic scattering in a large momentum transfer regime, i.e., Compton scattering. Comparison with *ab initio* local-density approximation calculations evidenced that a significant effect on the electronic density of Rb_4C_{60} was due to an unexpected overall contraction of the C_{60} molecule, which is itself under pressure.¹⁰ Such a C_{60} molecule contraction is surprising since calculations bring the bulk modulus of an individual molecule higher than that of a diamond.¹¹

Raman scattering is known to be particularly suitable in probing phase transitions, structural ordering, and charge transfer from the alkali dopant to the C_{60} molecule.¹² In this paper, we report the results of high pressure Raman spectroscopy

study of Rb_4C_{60} at room temperature with pressures up to 8 GPa. The following points motivated our work: (i) probing the transition around 0.8 GPa, and possibly distinguishing between the electronic and the structural origins of the transition. In particular, testing the relevancy of the Compton scattering results about the contraction of the molecule. (ii) Studying the effect of pressure on vibrational frequencies as a function of the applied pressure for pressures higher than the insulator to metal transition around 0.8 GPa.

II. EXPERIMENT PROCEDURE

Rb_4C_{60} was produced by a solid-solid reaction between weighted quantities of purified C_{60} and synthesized Rb_6C_{60} . Saturated phase Rb_6C_{60} was produced by using a vapor-transport method.¹³ The reaction is carried out in a vacuum-sealed Pyrex glass tube for at least two months. The evolution of the reaction is controlled by x-ray diffraction until the complete reaction of Rb_6C_{60} and, hence, its disappearance. We observed no impurities in the studied sample.

In a glove box, the sample was loaded in a membrane diamond anvil cell¹⁴ (MDAC) using a stainless steel gasket with a 350 μm diamond culet using neon as the pressure transmitting medium.¹⁵ This pressure transmitting medium ensures quasihydrostatic conditions on the sample. The R1-line emission of a tiny ruby¹⁶ was used for pressure calibration.¹⁷ The Raman experiments were carried out at 300 K using a triple monochromator Jobin Yvon T64000 in a back scattering configuration. The power of the 514.5 nm (2.41 eV) radiation from an argon-ion laser was measured directly on the MDAC and was always kept below 2 mW in front of the window in order to avoid any photoinduced transformation of the sample. The laser spot diameter on the sample was 5 μm . The Raman spectra, excited at 514.5 nm, were recorded.

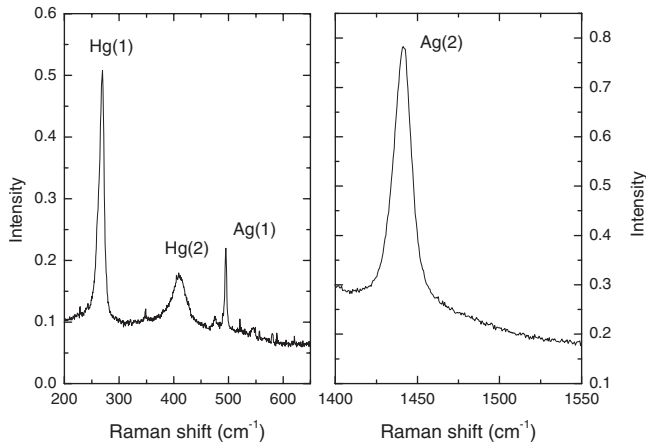


FIG. 1. Raman spectrum of Rb_4C_{60} measured at 0.25 GPa. The intramolecular modes are induced.

In these experiments, the pressure was increased up to 8 GPa.

III. RESULTS

The Raman spectra of Rb_4C_{60} were measured in two frequency regions from 30 to 1300 cm^{-1} and from 1380 to 1600 cm^{-1} in order to avoid the Raman mode of diamond at 1333 cm^{-1} . Due to the weak Van der Waals bonds interconnecting the C_{60} molecules in the doped fullerenes, the main effect of the alkali-metal doping of C_{60} is the charge transfer from metal to C_{60} molecule, i.e., to the lowest unoccupied molecular orbital. Compared to a pristine solid, it results in an expansion of the C_{60} molecule diameter linked to a softening of the intramolecular bonds within the C_{60} ball. In spite of both the C_{60} ball expansion and the lattice modifications due to intercalation, an overall similarity between the doped alkali-metals C_{60} and the pristine C_{60} spectra is established. The doping-induced changes in the Raman-active intramolecular modes has been exhaustively reviewed by Dresselhaus *et al.*¹²

The specific case of Rb_4C_{60} obeys this overall similarity since we observe the ten Raman-active lines predicted by group theory for the C_{60} molecule in icosahedral symmetry (i.e., two nondegenerate Ag and eight fivefold degenerate Hg), at positions corresponding to those observed in a previous Rb_4C_{60} Raman study at ambient pressure.¹⁸ Figure 1 shows our Raman spectrum of Rb_4C_{60} at 0.25 GPa, which is the starting pressure point. We will focus our study on the main intense intramolecular modes. The line at 1441 cm^{-1} is attributed to the tangential double-bond stretching pentagon pinch Ag(2) intramolecular mode. The position of the Ag(2) mode, compared to the pristine C_{60} , follows the rule of approximately 6 cm^{-1} softening per transferred electron, as observed in previous studies in K_xC_{60} (Refs. 12 and 19) or Rb_xC_{60} (Refs. 18 and 20), reflecting the lengthening of the C-C bonds due to intercalation. The Ag(1) radial breathing intramolecular mode is observed at 494 cm^{-1} in C_{60} fullerite consistently with the fact that this mode frequency is only slightly affected by doping (a balance between the mode softening due to the charge transfer to the C_{60} molecule and

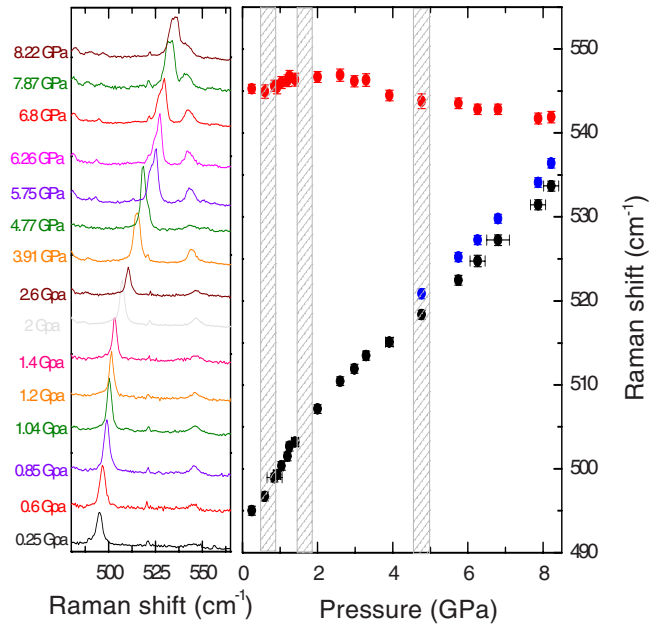


FIG. 2. (Color online) Evolution of Ag(1) and 545 cm^{-1} intramolecular modes between 0.25 and 8 GPa measured at room temperature. The vertical dashed lines indicate domains where the pressure induced changes are established.

the mode stiffening due to the electrostatic interaction between C_{60} molecule and rubidium atoms²¹). The line at 268 cm^{-1} corresponds to the Hg(1) intramolecular mode referring to the pristine C_{60} . Nevertheless, whereas C_{60} exhibits for Hg(1) a symmetric line well described with a Lorentzian shape, Rb_4C_{60} line displays a shoulder. The fitting of this line thus requires both a Lorentzian shape centered at 269 cm^{-1} and, as a result of electron-phonon coupling, a Breit-Wigner-Fano (BWF) shape centered at 264 cm^{-1} . Such a splitting has already been described for A_6C_{60} compounds and attributed to crystal field effects due to the alkali metal giving rise to polarization effects.²² The line at 409 cm^{-1} is attributed to Hg(2) intramolecular modes and is downshifted by 20 cm^{-1} compared to C_{60} due to the charge transfer between rubidium and carbon. The Hg(2) line is broad and asymmetric, and well described by a BWF line shape, indicating strong electron-phonon coupling as is usual in alkali doped C_{60} compounds.²³ In addition to these allowed Raman modes, we will also follow the mode at 545 cm^{-1} , which is not as observable in cubic C_{60} or C_{60} compounds as, for example, A_3C_{60} or A_6C_{60} . At this frequency, no Raman-active mode is expected in C_{60} . In Rb_4C_{60} compounds, a lowering in the structural symmetry due to intercalation and, thus, doping makes active grade Raman modes in addition to the ten Ag and Hg molecular active modes.¹² A tentative assignment of this mode could be the F_{1g} symmetry mode.²⁴

We now examine the pressure dependence of these modes.

In Fig. 2, we follow the evolution of Ag(1) and F_{1g} modes between 0.25 and 8 GPa at room temperature. For memory, Ag(1) mode corresponds to the breathing of the C_{60} molecule. In Fig. 2(a), one observes an overall frequency upshift in the Ag(1) mode and its splitting in two branches at high

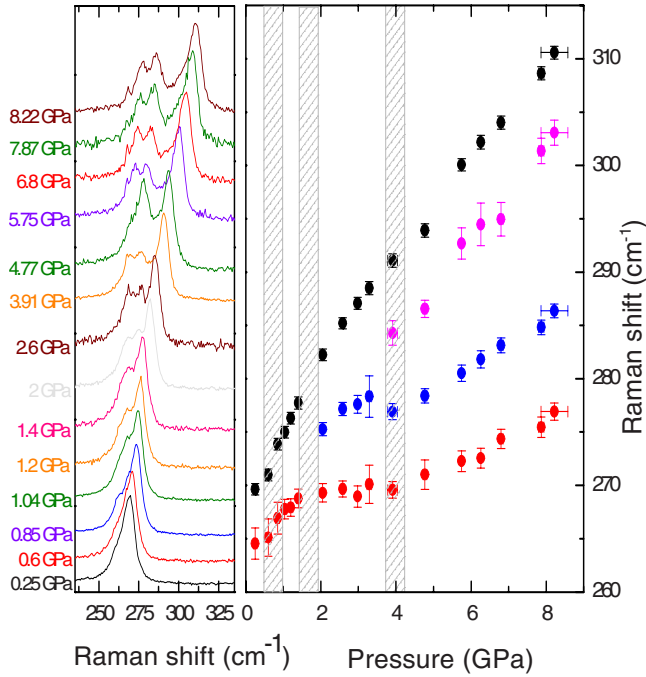


FIG. 3. (Color online) Evolution of Hg(1) intramolecular mode between 0.25 and 8 GPa measured at room temperature. The vertical dashed lines indicate the domains where the pressure induced changes are established.

pressure with the relative weight of these two bands becoming equal around 8 GPa. Meanwhile, the F_{1g} mode undergoes an overall frequency downshift accompanied by a reinforcement of its relative weight. To examine the behavior of these modes more precisely on Fig. 2(b), the Ag(1) mode exhibits a slight change at 0.6 GPa where the slope $d\omega/dP$ (estimated from the first two points) of 4.8 $\text{cm}^{-1}/\text{GPa}$ increases to 8.2 $\text{cm}^{-1}/\text{GPa}$ up to around 2 GPa. This slope then decreases to 4.2 $\text{cm}^{-1}/\text{GPa}$ up to 4 GPa, beyond which the splitting occurs into two very close branches. To refer to the C_{60} mode under pressure,^{25,26} we mention that the Rb₄C₆₀ Ag(1) mode exhibits quite a different behavior. We observe (i) no frequency softening at low pressure, whereas C_{60} exhibits such a softening below 0.4 GPa due to the pressure induced fcc to the partially ordered simple cubic phase transition;²⁶ (ii) a transition pressure at 2 GPa instead of the 2.5 GPa in C_{60} , which is attributed to a rotation-free C60 structurally ordered phase; and (iii) a splitting of modes at high pressure, which is absent in C_{60} . The reader can refer to the detailed review of the fullerene behavior under pressure, which was done by Sundqvist.²⁷

The F_{1g} mode presents a particular behavior with respect to other intramolecular modes. Its frequency is constant up to 0.6 GPa and then increases up to a maximum around 1.5 GPa. It then remains constant up to 2.6 GPa and then undergoes a gradual decrease after 3 GPa up to 8 GPa. The pressure dependence of both Ag(1) and F_{1g} modes indicates that these two modes would cross around 10 GPa.

The pressure dependence of the low frequency Hg(1) mode is shown in Fig. 3. This symmetry is characterized by a mixed radial and tangential behavior.¹² As already pointed out, the starting pressure point already presents two modes

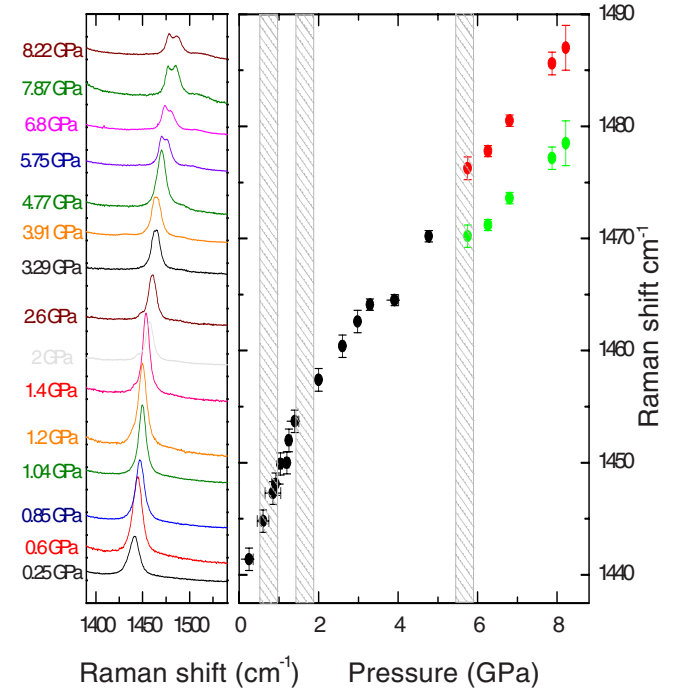


FIG. 4. (Color online) Evolution of Ag(2) intramolecular mode between 0.25 and 8 GPa at room temperature. The vertical dashed lines indicate the domains where the pressure induced changes are established.

instead of one for C_{60} . The frequency of these two lines is downshifted respectively by 7 and 4 cm^{-1} , which is compared to the C_{60} one as a consequence of the charge transfer. Figure 3(a) shows the occurring splittings around 2 and 4 GPa together with the observable transitions of the higher frequency mode at 0.6 and 2 GPa. In detailing the pressure dependence of these observed lines, we note that both of the lines present at low pressure show a change of slope around 0.6 GPa. The lower frequency mode around 264 cm^{-1} presents a slope of 1.6 $\text{cm}^{-1}/\text{GPa}$ below 0.6 GPa and then a slope of 4.3 $\text{cm}^{-1}/\text{GPa}$ until 1.7 GPa. It then reaches a plateau before increasing again with the pressure after 4 GPa. The higher frequency line around 269 cm^{-1} exhibits first a slope of 3.8 $\text{cm}^{-1}/\text{GPa}$ below 0.6 GPa and then a slope of 7 $\text{cm}^{-1}/\text{GPa}$ until 1.7 GPa. Its slope downshifts to 4.7 $\text{cm}^{-1}/\text{GPa}$ and remains continuous until 8 GPa. Around 2 GPa, a new line appears exhibiting a slope of 2.4 $\text{cm}^{-1}/\text{GPa}$. This new line splits again into two branches around 4 GPa. The lowest of these new branches exhibits a slope around 2.1 $\text{cm}^{-1}/\text{GPa}$ while the higher frequency one exhibits a slope of 4.4 $\text{cm}^{-1}/\text{GPa}$. The difference with the C_{60} case is drastic since the C_{60} Hg(1) mode goes above 0.4 GPa, i.e., after the orientational ordering, a continuous frequency upshift occurs.^{25,26}

Figure 4 displays the pressure dependence of the so-called pentagonal pinch Ag(2) mode that involves out of phase pentagonal ring contraction and hexagonal ring dilatation, which is characterized by tangential displacements. Figure 4(a) shows a continuous overall frequency upshift of the mode. Figure 4 shows neither a clear evidence of the transition around 0.6 GPa nor of the transition around 1.7 GPa. At

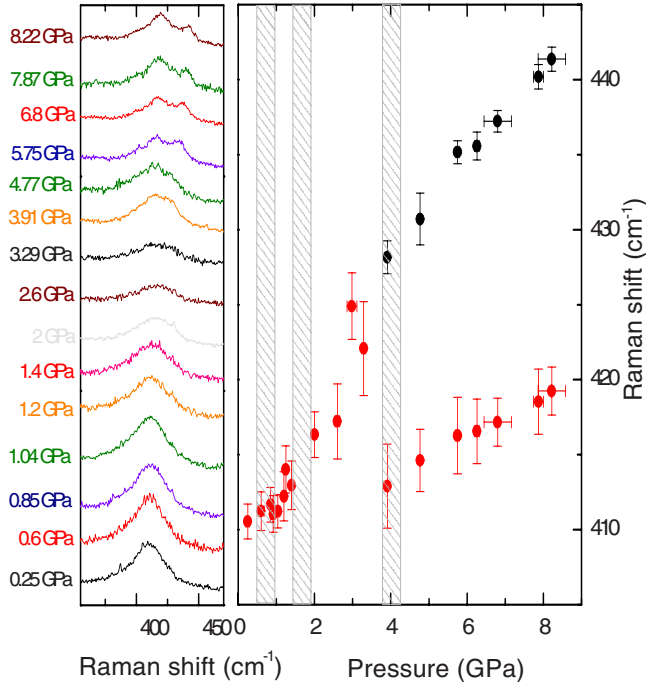


FIG. 5. (Color online) Evolution of Hg(2) intramolecular mode between 0.25 and 8 GPa at room temperature. The vertical dashed lines indicate the domains where the pressure induced changes are established.

higher pressure, the line splits into two branches. To more precisely detail the behavior of this mode, the slope $d\omega/dP$, whose value is $10.4 \text{ cm}^{-1}/\text{GPa}$ below 1.7 GPa, softens to become $5.3 \text{ cm}^{-1}/\text{GPa}$ above 1.7 GPa. An unhook in the frequency is observed around 4 GPa, becoming a splitting around 5 GPa. The intensity of the two branches is the same. Both of the branches follow a linear law with $3.4 \text{ cm}^{-1}/\text{GPa}$ for the lowest one and $4.5 \text{ cm}^{-1}/\text{GPa}$ for the highest one. In contrast, one can recall the C_{60} stable continuous pressure dependence $d\omega/dP=5.5 \text{ cm}^{-1}/\text{GPa}$ until 6 GPa.^{25,26}

Figure 5 shows the pressure dependence of the intramolecular Hg(2) that, as well as the Hg(1) mode, is characterized by a mixed radial and tangential behavior.¹² Figure 5(a) shows the hardening of the mode with the pressure together with its broadening. Its intensity drops down before the splitting is visible at 3.9 GPa. We also followed the broadening of the BWF line as a function of pressure. It undergoes a sharp increase around 0.6 GPa and reaches a maximum at 4 GPa. As a consequence, the electron–phonon coupling is enhanced around 0.6 GPa and reaches a maximum at 4 GPa before decreasing.

The Hg(2) mode is characterized by a slope of $1.9 \text{ cm}^{-1}/\text{GPa}$ between 0.25 and 0.8 GPa. The slope then increases up to around 1.7 GPa and undergoes another change to reach $5.8 \text{ cm}^{-1}/\text{GPa}$ before splitting into two branches.

In C_{60} , the pressure dependence of the Hg(2) mode is definitely different since it does not undergo any splitting until 7 GPa.

IV. DISCUSSION AND CONCLUSION

One can extract three main features in the pressure dependence of our Raman scattering measurements, corresponding to the pressures around 0.6, 1.7, and 4 GPa. We discuss them as follows.

A. Edge of 0.6 GPa

As already mentioned, two data points were obtained before 0.85 GPa and were used to calculate the slopes $d\omega/dP$ of the Hg(1), Ag(1), and F_{g1} modes. These slopes undergo a change at 0.6 GPa. Moreover, the Hg(2) mode becomes more asymmetric, indicating a more important electron–phonon coupling. These changes in the Raman spectra may be signatures of the vibrational and electronic modifications around 0.6 GPa. Such a modification would suggest a structural, as well as an electronic, transition. The diffraction results probe a structural transition around 0.6 GPa, which is consistent with the Raman scattering results. Sabouridodaran *et al.*⁸ attributed the structural modification to an isostructural transition conserving the tetragonal symmetry. This assumption is discussed by Huq and Stephens.⁹ Their recent detailed Rietveld refinement of the Rb_4C_{60} structure while under pressure evidences a phase change from tetragonal to orthorhombic symmetry between 0.4 and 0.8 GPa, which is related to an orientational disorder–order transition. The NMR results probe an insulator to metal electronic transition around 0.8 GPa, which is consistent with our results particularly for the Hg(2) mode. The upshift of intramolecular modes at low pressure is related to the strengthening of the C-C interaction. This is enhanced above 0.6 GPa. This observation in particular concerns the breathing Ag(1) mode and may support the assumption of C_{60} contraction as it is given by the Compton scattering results, which point to an unexpected 3% average volume contraction of the C_{60} molecule between 0.2 and 2 GPa. Nevertheless, it remains a difficult task to conclude clearly about this contraction due to the blending of the electronic and structural transition effects, and also to the few numbers of measured points in this domain of pressure.

B. Edge of 1.7 GPa

Our Raman observation indicates a change in the behavior of the intramolecular modes around 1.7 to 2 GPa. This result is consistent with the Rietveld refinement performed by Huq and Stephens. Their diffraction results allowed us to follow the lattice parameters as a function of pressure.⁹ The b parameter undergoes a decrease whereas the c parameter smoothly increases to intersect the b parameter at a pressure close to 1.7 GPa. The decrease in C_{60} - C_{60} , as well as the Rb-C distances combined to the frequency softening of Hg(1), Ag(1), and Ag(2) modes, leads to a picture of higher electron hopping in this domain of pressure.

C. Edge of 4 GPa

Around 4 GPa, all Raman lines present important changes. All intramolecular modes undergo huge modifications at this pressure, as already described above. If we refer

to the structural change of the C₆₀ molecule when isolated, it possesses Ih symmetry. When placed into a crystal, the C₆₀ molecule undergoes a lowering in its symmetry and, according to Klupp *et al.*,²⁸ molecular symmetry is D_{2h}. Nevertheless, we do not observe, at ambient pressure, the expected splitting of intramolecular modes given by the group theory for D_{2h}. For example, we observe only partial splitting for Hg(1) since we get two components at ambient pressure, then three around 2 GPa, and then four branches around 4 GPa. The Ag(2) and Hg(2) modes undergo a splitting around 4 GPa. These results suggest a clear lowering in the C₆₀ molecule symmetry around this pressure: the C₆₀ cage undergoing a higher structural deformation making the activation of the new observed modes possible. The polymerization could explain such a C₆₀ cage deformation, but we can rule out such polymerization, i.e., breaking of double bonds through the formation of rings joining two C₆₀ molecules, for the following reasons. First, we do not observe any mode appearing around 1000 cm⁻¹, which is considered as a Raman fingerprint for such intermolecular bonds.²⁹ Moreover, the Ag(2) mode downshifts by 5 cm⁻¹ per polymer bond:^{29,30} we do not observe such a downshift but splitting. A structural phase transition occurring around 4 GPa would also cause the C₆₀ molecule deformation. Such a transition has not been reported in a diffraction study⁸ that measured Rb₄C₆₀ from an ambient pressure to 5.2 GPa. Nevertheless, we may attribute the lack of any observation of this transition to the fact that the Rb₄C₆₀ sample was a three phase assemblage so that the authors were not able to refine the entire diffraction

pattern even at low pressure but focused on a short number of low order peaks.

To conclude, the richness of the Rb₄C₆₀ compound offers three major changes in the vibrational frequencies up to 8 GPa. The structural, as well as electronic, transition at 0.6 GPa drive the behavior of the observed modes. It seems difficult to distinguish between the electronic and the structural origins of this transition, and to address the possible contraction of C₆₀ molecules. Molecular dynamics calculations, taking into account applied pressure, would help assign the origin of the transition. The second set of features observed around 1.7–2 GPa correspond to the pressure induced structural rearrangement leading mainly to higher electron hopping. The third and unexpected change is observed around 4 GPa. The observation of the clear variation through the frequency upshift or the splitting of all modes leads to invoke a reduction in the symmetry of the C₆₀ molecule that maybe accompanied by a structural phase transition, which would cause the deformation of the C₆₀ cage. Moreover, we found no evidence for any polymerization until 8 GPa. Such a result may enhance the interest for a new diffraction study for pressures higher than 2 GPa to clear the structural behavior of Rb₄C₆₀ under high pressure.

ACKNOWLEDGMENTS

We are pleased to thank Bernard Canny and Pascal Munch for their kind help, Frédéric Datchi, Abhay Shukla, Massimiliano Marangolo, and Geneviève Loupias for enlightening discussion.

-
- ¹S. C. Erwin, in *Buckminsterfullerenes*, edited by W. E. Billups and M. A. Ciufolini (VCH, New York, 1993), p. 217; P. J. Benning, Jose Luis Martins, J. H. Weaver, L. P. F. Chibante, and R. E. Smalley, *Science* **252**, 1417 (1991).
- ²R. M. Fleming, M. J. Rosseinsky, A. P. Ramirez, D. W. Murphy, J. C. Tully, R. C. Haddon, T. Siegrist, R. Tycko, S. H. Glarum, P. Marsh, G. Dabbagh, S. M. Zahurak, A. V. Makhija, and C. Hampton, *Nature (London)* **352**, 701 (1991).
- ³O. Chauvet, G. Oszlanyi, L. Forro, P. W. Stephens, M. Tegze, G. Faigel, and A. Janossy, *Phys. Rev. Lett.* **72**, 2721 (1994).
- ⁴S. C. Erwin and M. R. Pederson, *Phys. Rev. Lett.* **67**, 1610 (1991).
- ⁵M. Capone, M. Fabrizio, P. Giannozzi, and E. Tosatti, *Phys. Rev. B* **62**, 7619 (2000).
- ⁶G. Klupp, K. Kamaras, N. M. Nemes, C. M. Brown, and J. Leao, *Phys. Rev. B* **73**, 085415 (2006); K. Kamaras, G. Klupp, D. B. Tanner, A. F. Hebard, N. M. Nemes, and J. E. Fischer, *ibid.* **65**, 052103 (2002).
- ⁷G. Zimmer, M. Elme, M. Mehring, and F. Rachdi, *Phys. Rev. B* **52**, 13300 (1995).
- ⁸A. A. Sabouri-Dodaran, M. Marangolo, C. Bellin, F. Mauri, G. Fiquet, G. Loupias, M. Mezouar, W. Crichton, C. Hérold, F. Rachdi, and S. Rabii, *Phys. Rev. B* **70**, 174114 (2004); December 13, 2004 issue of *Virtual journal of nanoscale Science & Technology* (<http://www.vjnano.org>).
- ⁹A. Huq and P. W. Stephens, *Phys. Rev. B* **74**, 075424 (2006).
- ¹⁰A. A. Sabouri-Dodaran, C. Bellin, M. Marangolo, G. Loupias, S. Rabii, Th. Buslaps, M. Mezouar, F. Rachdi, *Phys. Rev. B* **72**, 085412 (2005).
- ¹¹R. S. Ruoff and A. L. Ruoff, *Nature (London)* **350**, 663 (1991); S. J. Woo, S. H. Lee, E. Kim, K. H. Lee, Y. H. Lee, S. Y. Hwang, and I. C. Jeon, *Phys. Lett. A* **162**, 501 (1992); B. Sundqvist, *Adv. Phys.* **48**, 1 (1999).
- ¹²M. S. Dresselhaus, G. Dresselhaus, and P. C. Ecklund, *J. Raman Spectrosc.* **27**, 351 (1996).
- ¹³C. Hérold, J. F. Marêché, and P. Lagrange, *C. R. Acad. Sci. Paris, Ser. Iib* **321**, 103 (1995).
- ¹⁴J. C. Chervin, B. Canny, J. M. Besson, and Ph. Pruzan, *Rev. Sci. Instrum.* **66**, 2595 (1995).
- ¹⁵B. Couzinet, N. Dahan, G. Hamel, and J. C. Chervin, *High Press. Res.* **23**, 409 (2003).
- ¹⁶J. C. Chervin, B. Canny, and M. Mancinelli, *High Press. Res.* **21**, 305 (2001).
- ¹⁷D. Barnett, S. Block, and G. J. Piermarini, *Rev. Sci. Instrum.* **44**, 1 (1973).
- ¹⁸M. G. Mitch and J. S. Lannin, *Phys. Rev. B* **51**, 6784 (1995).
- ¹⁹P. Dahlke, P. F. Henry, and M. Rosseinsky, *J. Mater. Chem.* **8**, 1571 (1998).
- ²⁰M. G. Mitch and J. S. Lannin, *J. Phys. Chem. Solids* **54**, 1801 (1993).

- ²¹R. A. Jishi and M. S. Dresselhaus, *Phys. Rev. B* **45**, 6914 (1992).
- ²²P. Zhou, K. A. Wang, Y. Wang, P. C. Ecklund, M. S. Dresselhaus, G. Dresselhaus, and R. A. Jishi, *Phys. Rev. B* **46**, 2595 (1992).
- ²³P. Zhou, K. A. Wang, P. C. Ecklund, and M. S. Dresselhaus, *Phys. Rev. B* **48**, 8412 (1993).
- ²⁴P. H. M. van Loosdrecht, P. J. M. van Bentum, M. A. Verheijen, and G. Meijer, *Chem. Phys. Lett.* **198**, 587 (1992).
- ²⁵D. W. Snoke, Y. S. Raptis, and K. Syassen, *Phys. Rev. B* **45**, 14419 (1992).
- ²⁶K. P. Meletov, D. Christofilos, S. Ves, and G. A. Kourouklis, *Phys. Rev. B* **52**, 10090 (1995).
- ²⁷B. Sundqvist, *Adv. Phys.* **48**, 1 (1999).
- ²⁸G. Klupp, K. Kamaras, N. M. Nemes, C. M. Brown, and J. Leao, *Phys. Rev. B* **73**, 085415 (2006).
- ²⁹T. Wagberg, P. Stenmark, and B. Sundqvist, *J. Phys. Chem. Solids* **65**, 317 (2004).
- ³⁰V. A. Davidov, L. S. Kashevarova, A. V. Rakhmanina, V. M. Senyavin, R. Céolin, H. Szwarc, H. Allouchi, and V. Agafonov, *Phys. Rev. B* **61**, 11936 (2000).